

# Allowable Shears for Plastered Straw-Bale Walls

M. Aschheim<sup>1</sup>; S. Jalali<sup>2</sup>; C. Ash<sup>3</sup>; K. Donahue<sup>4</sup>; and M. Hammer<sup>5</sup>

**Abstract:** Although straw-bale construction originated in the midwestern United States in the late 1800s, the engineering of plastered straw-bale walls to resist in-plane lateral loads is a modern development. Relevant experimental studies are reviewed and allowable shears are developed for use in design for wind and seismic loading. Clay, soil-cement, lime, lime-cement, and cement plasters having various thicknesses and reinforced with welded steel wire mesh, woven steel wire mesh, or polypropylene mesh are considered. Experimental values are adjusted on the basis of moment-curvature analysis results to account for lower-bound model code material strengths, plaster thicknesses, and mesh reinforcement. A conventional model for shear strength is used to provide a preliminary assessment of true shear strength. The resulting design values and associated detailing requirements are summarized in a format suitable for implementation in model code provisions for straw-bale construction. DOI: [10.1061/\(ASCE\)ST.1943-541X.0001101](https://doi.org/10.1061/(ASCE)ST.1943-541X.0001101). © 2014 American Society of Civil Engineers.

## Introduction

Straw-bale construction originated in Nebraska in the late 1800s, shortly after the invention of baling machines. Some of these early buildings, more than 100 years old, are still in service. After many decades of quiescence, straw-bale construction enjoyed a rebirth in the American southwest during the 1980s. Interest in this rediscovered building method has grown rapidly, in part owing to the economic and environmental sustainability inherent in using a low-cost construction material that has excellent thermal properties and which is obtained as a by-product of food production. Straw from wheat, rice, barley, and other grains typically is baled in the field, after harvest, using agricultural equipment that packs the straw tightly into consistent rectangular blocks. Two or three strings, typically polypropylene string or baling wire, maintain the compressed straw in the baled configuration.

Straw-bale buildings exist in 49 of the 50 states in the United States. Variations of straw-bale construction are practiced in more than 45 countries, in virtually every climate. There are more than 600 straw-bale buildings in California alone, including areas having considerable seismic exposure. Residences, schools, office buildings, and wineries have been built in the United States, including multistory buildings and buildings with floor areas greater than 10,000 ft<sup>2</sup> (930 m<sup>2</sup>). In many of these structures, straw-bale walls are used as load-bearing elements or shear walls. As shear walls, the straw-bale walls are often used as infill elements within a post and beam frame. Use as load-bearing walls is not uncommon, with loads applied at the top of the plastered straw-bale wall by means of a plywood box beam. Such loads are delivered, directly or

indirectly, into the relatively stiff plaster skins. Any mesh used to reinforce the plasters typically is stapled to wood members at the top and bottom of the wall. Good detailing practice involves use of generous roof overhangs to limit exposure to wind-driven rain and the use of vapor-permeable plasters to allow the bales to dry, in the event that moisture enters the wall assembly. Comprehensive, state-of-the-art guidance addressing structural, moisture control, fire resistance, and durability aspects of straw-bale construction is provided by King et al. (2006).

In the United States, building code provisions or guidelines exist in at least six cities and five counties, and in the states of California, New Mexico, and Oregon (Hammer et al. 2006). However, little guidance is available in these documents for establishing design strengths for in-plane resistance to lateral forces. Consequently, most buildings utilizing straw-bale walls as lateral force resisting elements have been permitted under the alternative means and methods provisions of the applicable building code.

Experimental tests of the lateral load response of straw-bale wall assemblies are relatively few in number. Tests conducted by some of the authors as part of a comprehensive testing program coordinated by the Ecological Building Network and relevant tests conducted in other testing programs are summarized herein and used as a basis for the development of allowable shear values. Results obtained from these tests were used to derive braced panel lengths for straw-bale walls in the Straw-Bale Construction appendix approved for inclusion in the 2015 International Residential Code.

## Summary of Relevant In-Plane Experimental Tests

The most relevant tests of plastered straw-bale walls subjected to in-plane loading are summarized below.

### Infilled Post-and-Beam Walls Tested by Ramirez

Ramírez (1999) reports the results of two 8-ft (2.44-m) high by 8-ft (2.44-m) long specimens built using a cement plaster (stucco) on one side of the wall and gypsum plaster on the other side. In each case the plaster was reinforced with 17-gauge (1.37-mm) galvanized woven wire stucco netting. Each wall was bounded by post and beam framing; in Unit One, three-string bales were used, and only the bales were directly confined by the post and beam framing; for Unit Two, two-string bales were used, and the plaster

<sup>1</sup>Professor and Chair, Dept. of Civil Engineering, Santa Clara Univ., 500 El Camino Real, Santa Clara, CA 95053 (corresponding author). E-mail: [maschheim@scu.edu](mailto:maschheim@scu.edu)

<sup>2</sup>Graduate Student, Santa Clara Univ., 500 El Camino Real, Santa Clara, CA 95053.

<sup>3</sup>Associate Principal, Degenkolb Engineers, 600 University St., Suite 720, Seattle, WA 98101; formerly, Graduate Student, Dept. of Civil Engineering, Univ. of Illinois, Urbana, IL 61801.

<sup>4</sup>Structural Engineer, 1101 8th St. #180, Berkeley, CA 94710.

<sup>5</sup>Architect, 1348 Hopkins St., Berkeley, CA 94702.

Note. This manuscript was submitted on January 4, 2013; approved on April 17, 2014; published online on July 1, 2014. Discussion period open until December 1, 2014; separate discussions must be submitted for individual papers. This technical note is part of the *Journal of Structural Engineering*, © ASCE, ISSN 0733-9445/06014008(9)/\$25.00.

facings were directly confined (in bearing) by the post and beam framing.

### Load-Bearing Walls Tested by Ash

Ash et al. (2003) report results of six full-scale specimens [nominally 8-ft (2.44-m) high by 8-ft (2.44-m) long]. The walls were made with three-string rice bales. Clay plaster was used on three walls, and a cement-lime plaster was used on the other three walls. The clay plasters were reinforced with polypropylene baling twine, polypropylene mesh, or welded wire mesh, whereas the cement-lime plasters were reinforced with woven wire mesh or welded wire mesh. Each series of three walls was conceived to represent a range of details derived from the preferences of a variety of builders, considering the results of substantial investigations into the behavior of materials and details in so-called *small* and *medium* scale tests. Consequently, the tests aimed to discriminate among the best alternatives envisioned at the time. The plasters themselves are near the extremes of weak and strong plasters, whereas the details represent *low*, *medium* and *high* levels of detailing.

Of the walls subjected to reversed cyclic inelastic loading, two clay plaster wall assemblies (Wall B, using welded wire mesh reinforcement, and Wall C, using polypropylene mesh reinforcement) and one cement plaster assembly (Wall E, using welded wire mesh reinforcement) were considered to have the best inelastic behavior relative to that obtained using the materials and detailing provided in the other walls that were tested. Thus, the reinforcement and detailing of these tests forms the basis of the model code requirements (Hammer et al. 2013) and associated allowable shear values.

The test setup is shown in Fig. 1. In-plane lateral load was applied by means of a hydraulic actuator. Vertical load was applied at the top of the walls to approximate a uniform load along the top of the wall equal to 200 lbf/ft (2.92 kN/m). This is considered to be on the light side of the dead load to be expected from a roof in single story load-bearing construction. Because the lateral load was applied by means of a heavy steel tube section running along the top of the beam, a system of counterweights was devised to achieve the 200 lbf/ft (2.92 kN/m) loading.

The clay and cement-lime plasters were each nominally 1-1/2-in. (38.1-mm) thick. The clay plaster was comprised of clay, sand, water, and straw fibers. Compression tests of 2-in. (50.8-mm) cube samples yielded an average compressive strength of 290 psi (2.00 MPa) after curing for 44 days in the laboratory. This value is considered representative of the plaster strength at the time the walls were tested.

The cement-lime plaster (also known as *stucco*) was mixed in a mortar mixer using the following quantities (by volume measure):

30 gal. of sand (114 L), 8 gal. (30.3 L) of cement, 2 gal. (7.6 L) of slaked lime, and 6-1/2 gal. (24.6 L) of water. The lime had been hydrated prior to mixing by mixing in 6 gal. (22.7 L) of water per 50 lb (22.7 kg) bag of slaked finish lime. This mixture was allowed to hydrate for five days until the lime ceased absorbing water. At seven days, a three-cube set of cement plaster had an average strength of 1,850 psi (12.8 MPa). At 36 days, three cubes from the same batch had an average strength of 2,210 psi (15.2 MPa), whereas another set of three cubes from the same batch had a strength of 2,200 psi (15.2 MPa) at 95 days. A value of 2,200 psi (15.2 MPa) is considered representative of the plaster strength at the time the walls were tested.

Three-string rice straw bales were used, having nominal dimensions of 16 × 24 × 48 in. (410 × 610 × 1,220 mm), ordered as height, depth, and width, respectively.

Each of these wall specimens was subjected to reversed cyclic loading as defined in Fig. 2, which plots drifts of up to 5% [4.92 in. (125 mm) at the top of the wall]. The lateral force applied at the top of the wall and corresponding displacement, for the each wall, is plotted in Fig. 3. It should be noted that two complete cycles of displacement to ±7% drift were applied subsequently, under manual control.

Wall B was designed and built with a polypropylene reinforcing mesh. The mesh was anchored using 16-gauge (1.59-mm) 1-1/4-in. (31.8-mm) leg 7/16-in. (11.1-mm) crown staples applied diagonally over every mesh intersection. During testing, the predominant failure mode observed was compression zone crushing and base sliding, with the base sliding becoming more pronounced at later stages of the test. The peak capacity of 4.7 kips (20.9 kN) was reached on the 8th load step, at a drift level of 1% (0.96 in. or 24.3 mm). The change in the shape of the hysteresis loops [Fig. 3(a)] with increasing displacements may indicate that sliding of the wall becomes more significant at higher displacements. Manual measurements taken to assess the sliding behavior indicated 3/4 in. (19.1 mm) amplitude (peak to peak) of slip during load step 14 (4% drift), accounting for 20% of the actuator displacement at this amplitude. Working of the polypropylene mesh and compression at the base of the plaster were observed to wear down the earth plaster, gradually reducing it to its sand, clay, and straw components. This wearing and crushing caused an apparent reduction in the height of the wall. The soil debris at the base of the wall functioned as a wedge to push the plaster out of plane, away from the bales, in the portion of the cycle in which the plaster was loaded in compression. Nevertheless, relatively ductile behavior was apparent in the load-displacement plot.



Fig. 1. Overview of full-scale test setup used by Ash et al. (2003)

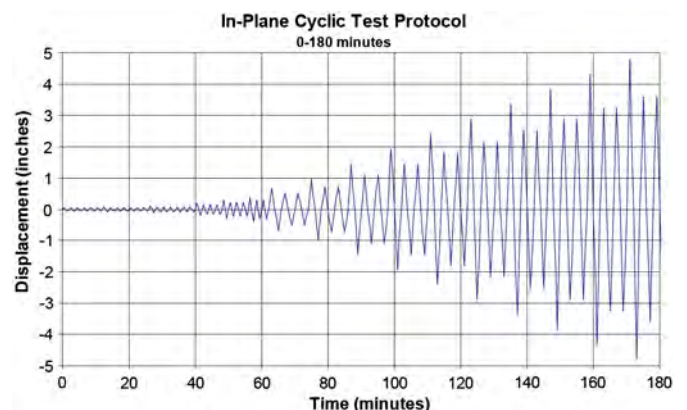
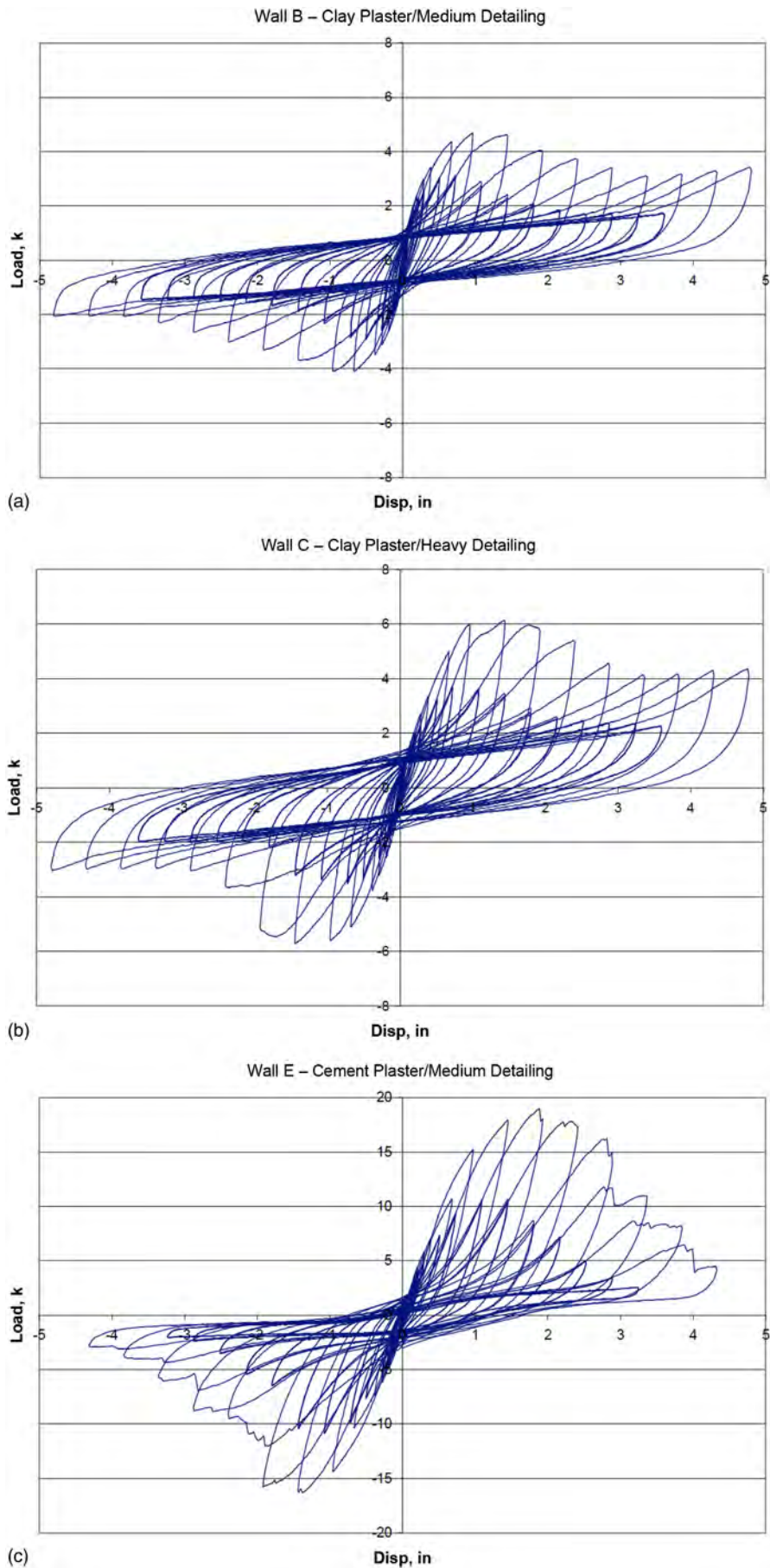


Fig. 2. Reversed cyclic loading protocol to 5% drift (4.92 in.)



**Fig. 3.** Load-displacement plot for (a) Wall B; (b) Wall C; (c) Wall E

Wall C used a heavy 2 × 2-in. (51 × 51-mm) 14-gauge (2.03-mm) wire mesh, anchored in place with 16-gauge (1.59-mm) 1–1/4-in. (31.8-mm) leg 7/16-in. (11.1-mm) crown staples placed diagonally over every mesh intersection. The first course of bales was anchored to the base through plywood plates and threaded rods. As shown in Fig. 3(b), these modifications resulted in an increase in the lateral strength of this wall relative to that of Wall B, with a peak load of 6.1 kips (27.1 kN) occurring at 1.5% drift (1.44 in., or 36.6 mm). At 1% drift, the 6.0 kip (26.7 kN) resistance was an increase of nearly 30% over the corresponding resistance of Wall B at this drift level. The overall response of this wall was similar to that of Wall B, with predominant failure modes consisting of crushing of the earth plaster and sliding of the wall at its base. The heavier mesh was observed to reduce the slip at the base of Wall C from a peak-to-peak amplitude of 3/4 in. (19 mm) in Wall B to 1/2 in. (13 mm) amplitude in this specimen at a drift of 4%. No flexural tension cracks were observed during testing of Wall C, suggesting the wire mesh created an *over-reinforced* condition in the sense that this word is used in reinforced concrete.

Wall E, the medium-detailed cement-lime plaster wall also used the 2 × 2-in. (51 × 51-mm) 14-gauge (2.03-mm) mesh, anchored with 16-gauge (1.59-mm) 1–3/4-in. (44.5-mm) leg 7/16-in. (11.1-mm) crown staples placed diagonally over mesh intersections. Through-ties running through the thickness of the wall and anchored by dowels in the body of the stucco were installed at every other course. (Note that through-ties are not considered necessary to reduce the likelihood of plaster buckling, because the plaster is well-adhered to the straw, and the straw provides lateral bracing to the plaster.) A 3.5 × 3.5-in. (89 × 89-mm) sill plate was used and was anchored at 2-ft (610-mm) centers. The combination of cement-lime plaster skins and the heavy wire mesh resulted in an increased lateral strength, having a peak value of 19 kips (84.5 kN) at 2% drift, as shown in Fig. 3(c). Several flexural cracks developed within the bottom third of the wall height as shown in Fig. 4. Failure of the wall was attributable to loss of tensile capacity of the reinforcing mesh, from both mesh fracture and staple pull out, as shown in Fig. 5. The mesh fracture was attributed to a combination of tensile elongation and low-cycle fatigue associated with the load reversals, which appeared to work the vertical wires of



Fig. 4. Flexural cracks in Wall E (2.5% drift level)



Fig. 5. Wall E mesh failure (7.5% drift level)

the mesh. The mesh fractures predominately occurred at the staple locations with some fractures also occurring at the intersections of the horizontal and vertical wires, where the wires are spot welded together in the manufacturing of the mesh.

More generally, for in-plane behavior, the plaster provides high initial stiffness that can serve to limit peak displacement response; as inelastic behavior develops in the plaster, a relatively soft core comprising the bales themselves is able to tolerate substantial displacements. During the tests, the walls proved to be very stable for gravity loads, with no gravity load failures occurring. At the conclusion of the prescribed loading (Fig. 2), the walls were then tested under manual control for two cycles to drifts of  $\pm 7\%$ , which corresponded to the stroke limit of the actuator. Under manual control, the walls simply rocked, with the bale joints opening up and then closing again. No degradation in the gravity load support mechanisms was evident, and there seemed little point to applying additional cycles of load. The relatively wide bale core provides a stable base for resisting gravity loads and thus enables the bales to serve as a secondary or back up system. It seems likely that the walls could tolerate simultaneous orthogonal excitation without significantly compromising their ability to maintain support for gravity loads because of the relatively generous width of the bales; this was evident even in the shake table tests where a much thinner bale wall was used (further information on this system, tailored for Pakistan, is available at [http://nees.unr.edu/projects/straw\\_bale\\_house.html](http://nees.unr.edu/projects/straw_bale_house.html)).

### Slender Wall Tested by Faurot

Faurot et al. (2004) tested a short version of Wall E (described above). The Faurot wall was nominally 4 ft (1.22 m) long (in plan) and 8 ft (2.44 m) high, composed of rice straw bales having dimensions 15 × 24 × 48 in. (380 × 610 × 1,220 mm), ordered as height, depth, and width, respectively). It used 2 × 2-in. (51 × 51-mm) 14-gauge (2.03-mm) mesh, attached with 16-gauge (1.59-mm) 1–3/4 in. (44.5-mm) leg 7/16-in. (11.1-mm) crown staples. The nominal 1–1/2-in. (38.1-mm) thick cement-lime plaster consisted of 12 parts sand, 4 parts Portland cement, 1 part lime, and water.

The lateral loading protocol matched that given in Fig. 2. Unlike the Ash et al. (2003) tests, no superimposed vertical loads were applied to the Faurot et al. (2004) wall. The resulting lateral load-lateral displacement response is given in Fig. 6. The peak strength was 7,000 lbf (31.1 kN).

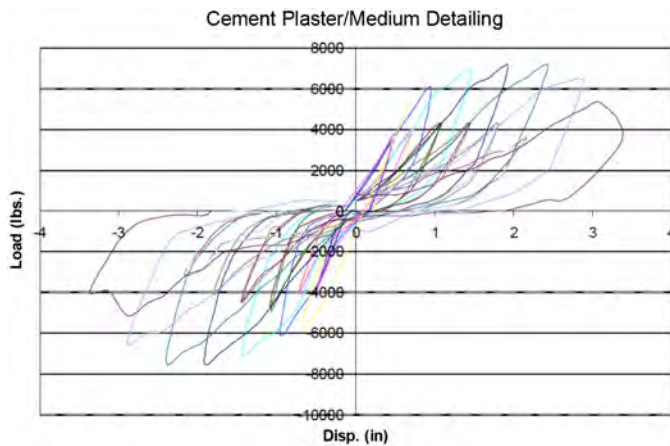


**Fig. 6.** Load-displacement response of slender wall tested by Faurot et al. (2004) (reprinted with permission from authors)

### Infilled Post-and-Beam Wall Tested by Nichols and Raap

Nichols and Raap (2000) report a test in which a shear failure was observed. This nominally 8-ft (2.44-m) by 8-ft (2.44-m) wall was built using cement plaster reinforced by a 2-in. (51-mm) by 2-in. (51-mm) 16-gauge (1.59-mm) welded wire mesh. A post and beam frame ran along the perimeter of the wall, and lag screws protruding from the post and beam frame provided for mechanical transfer of shear between the plaster and perimeter framing. Unlike the preceding tests, loads were applied monotonically. However, the test had to be repeated several times to reach failure.

### Development of Allowable Shears

Allowable shears are derived for the tested walls (B, C, and E) and extended to consider plasters of different strengths and mesh reinforcement. Conceptually, allowable shears could be based on strength or, for very flexible systems, may also consider deformation limits. Initial stiffnesses of reinforced straw-bale walls reported by Ash et al. (2003) ranged from 11.7–19.1 kip/in. (2,050–3,340 kN/m), which is similar to the range of 6.9–19.6 kip/in. (1,210–3,430 kN/m) determined from experimental tests of light-framed wood panel shear walls, as reported by Jalali et al. (2013, p. 30). Because the straw-bale walls have lateral stiffness comparable with that of wood panel shear walls, lateral stiffness need not be considered explicitly in establishing allowable shears. Thus, allowable shears are derived based solely on strength. It should be noted that the tested walls all displayed flexural failures; the true shear strengths, while not measured, are higher than the shears sustained in the development of flexural failures.

Ultimate strengths are taken as the average of the ultimate values in the first and third quadrants of the respective load-displacement plot. For Wall E, the average strength is 17.65 kips (78.51 kN); for Walls B and C, the averages are 4.40 and 5.93 kips (19.6 and 26.4 kN), respectively. Because the allowable shears are derived for use in both wind and seismic design, allowable values must be low enough to obtain elastic or nearly elastic behavior for wind load. Adjustments are made to account for the limited number of test specimens, the use of materials having strengths equal to the minimum values in the model code provisions, and differences in plaster thickness or reinforcement.

### Factors of Safety

Factors of safety were applied to develop allowable shears for allowable stress design (ASD). The CUREE-Caltech Wood-frame project reports that “tabulated ASD values that are currently used for seismic design of wood-frame shear walls are not based on the yield strength of the walls, but are instead based on an ultimate strength divided by a safety factor” [Consortium of Universities for Research in Earthquake Engineering (CUREE) 2004, p. 158–159]. Factors of safety for plywood walls vary from 2.5–3.1 and average 2.9. Thus, a factor of safety of 2.9 was applied to the ultimate strength for the cement plaster walls and other hard-skinned variants.

For a given load-displacement response, proportional changes in the factor of safety used to establish allowable shears and the  $R$  value used for seismic design have no effect on the resulting design. That is, one can use a lower  $R$  value together with a lower factor of safety (higher allowable shear) and achieve the same resulting design. Because it is desirable to use the same  $R$  value for the seismic design of straw-bale walls regardless of plaster type, a lower factor of safety, equal to 2.5, was used to establish the allowable shears for the clay plaster walls, which displayed greater ductility capacity. (This was considered preferable to using a larger  $R$  factor for straw-bale walls having clay plaster skins.)

### Adjustments for Plaster Thickness and Compressive Strength

All tested walls were nominally 8-ft (2.44-m) high and were tested as cantilevers restrained at the base. The height from the top of the sill to the centerline of the actuator is estimated as 107.5 in. (2.73 m), based on six bales each 16-in. (406-mm) high, a 5-1/2-in. (140-mm) high box beam, and half the height of the 12-in. (305-mm) high steel tube section used to apply load at the top of the box beam.

The plasters used in the test specimens, having mean cube compressive strengths of 2,200 psi (15.2 MPa) and 290 psi (2.0 MPa) for the cement and clay plasters are stronger than the baseline cube strengths (1,400 and 100 psi, or 9.7 and 0.69 MPa, respectively) established in the model code provisions. Just as for reinforced concrete walls with distributed reinforcement, flexural strengths could be estimated using a monotonic moment-curvature analysis (also known as a strain compatibility analysis) using the program *BIAX* (Wallace 1992). The reinforced plaster was analyzed, without consideration of the relatively small contribution of the bales to flexural strength.

Analyses for Wall E were made using a modulus of elasticity of plaster,  $E_p$ , taken as  $818 f'_p$ , where  $f'_p$  is the cube compressive

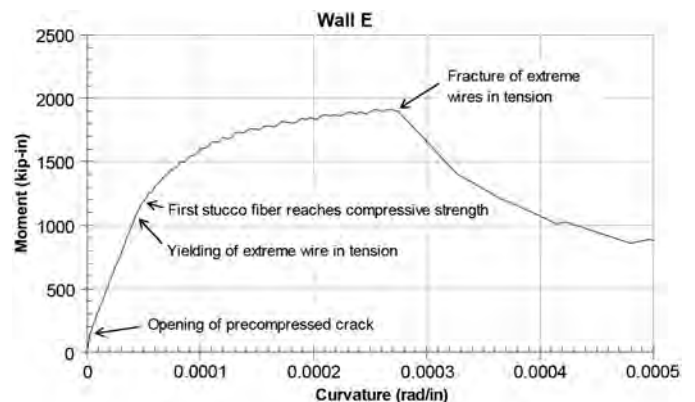


**Fig. 7.** Moment-curvature response for Wall E, computed using *BIAX*

strength of the plaster, and the strain at ultimate strength was taken as 0.0025, based on results presented by Vardy (2009). Parker et al. (2006) reports the mean strength of the mesh wire to be 384.2 lbf (1.71 kN) and this strength was represented in the *BIAX* model (rather than the lower strengths observed for unplastered meshes anchored by staples). A 5,000 lbf (22.2 kN) vertical load was applied at the top of the wall model, representing the estimated dead load and a superimposed load of 200 lbf/ft (2.9 kN/m). Using these assumptions, the moment-curvature response of was computed (Fig. 7). The flexural strength was determined to be 1,839 kip-in (208 kN-m), and this strength is equilibrated by an applied force (shear) of 19.2 kips (85.2 kN). This result compares well with the flexural strength of 19 kips (84.5 kN) obtained under reversed cyclic loading.

Moment-curvature analyses were used to account for changes in plaster thickness and the use of plasters having compressive strength equal to the baseline values. Allowable shears were reduced in proportion to the reduction in flexural strength determined from the strain compatibility analyses. Specifically, the so-called *hard* plasters considered in the model code provisions have minimum cube compressive strengths of 600, 1,000, and 1,400 psi (4.14, 6.89, and 9.65 MPa). Specified minimum plaster thicknesses of 7/8, 1, and 1.5 in. (22.2, 25.4, and 38.1 mm) were considered to result in average thicknesses of 1, 1–1/8, and 1–5/8 in. (25.4, 28.6, and 41.3 mm), respectively. Columns 7 and 8 of Table 1 report the associated adjustment factors. The modulus of elasticity used in the moment-curvature analyses of these hard plasters was determined as  $818 f'_p$ .

The model code provisions specify a minimum cube compressive strength of 100 psi (0.69 MPa) for clay plasters. The tendency of the moment-curvature analyses to greatly overestimate the lateral strength of Wall C (15.28 kips or 68.0 kN compared with 6.14 kips or 27.3 kN) is attributed to the relatively rapid degradation of the compression zone under repeated inelastic cyclic loading. Even so, a reduction in flexural strength would be expected as  $f'_p$  changes from 290 to 100 psi (1.99 to 0.69 MPa). The moment-curvature analyses indicate a flexural strength of 69.2% relative to that obtained with  $f'_p = 290$  psi (2.0 MPa). This reduction was applied to walls made with plaster designations A2 and A3.

### Adjustments for Mesh Cross-Sectional Area

16-gauge (1.59-mm) wire is drawn through finer dies and thus the smaller diameter wires tend to display a higher yield strength, attributable to strain hardening. For example, Parker et al. (2006) report mean strengths of 103.8 ksi (716 MPa) for 16-gauge (1.59-mm) mesh and 77.2 ksi (532 MPa) for 14-gauge (2.03-mm) mesh. To be conservative, however, the flexural strength expected for 16-gauge (1.59-mm) mesh reinforcement was taken at 60% of the strength of that applicable for the 14-gauge (2.03-mm) mesh, based simply on the reduction in cross-sectional area ( $0.003019 \text{ in.}^2/0.005026 \text{ in.}^2 = 1.948 \text{ mm}^2/3.243 \text{ mm}^2 = 0.60$ ).

Similarly, 17-gauge (1.37-mm) woven wire would be expected to have a yield strength greater than that of the tested 14-gauge (2.03-mm) mesh wires. As with the 16-gauge (1.59-mm) mesh, this potential increase in yield strength was ignored, and flexural strengths were taken as 72.9% of that obtained for 14-gauge (2.03-mm) mesh, based on both the reduction in cross sectional area and spacing of the wires ( $0.002290 \text{ in.}^2/0.005026 \text{ in.}^2 \times (2 \text{ in.}/1.25 \text{ in.}) = (1.477 \text{ mm}^2/3.243 \text{ mm}^2) \times (5.08 \text{ mm}/31.75 \text{ mm}) = 0.7290$  (Table 1).

**Table 1.** Development of Allowable Shears for Straw-Bale Walls

Designation	Plaster type	Plaster thickness (minimum, in.)	Plaster reinforcement (in.)	Unadjusted shear strength (kips)	Minimum cube strength (psi)	Adjustment factors		Adjusted shear strength (kips)	Factor of safety	Allowable shear, $V_{all}$ per foot (lbf/ft)		Shear strength $V_n$ (lbf/ft)	Factor of safety for shear
						Plaster	Mesh			Calculated	Proposed		
(1)	(2)	(3)	(4)	(5)	(6)	(7)	(8)	(9)	(10)	(11)	(12)	(13)	(14)
A1	Clay	1.5	none	1.36	100	0.937	1	1.27	2.5/0.9 = 2.78	57	60	720	12.0
A2	Clay	1.5	2 × 2 high-density polypropylene	4.40	100	0.692	1	3.05	2.5/0.9 = 2.78	137	140	1,280	9.1
A3	Clay	1.5	2 × 2 × 14 ga.	5.93	100	0.692	1	4.10	2.5/0.9 = 2.78	185	190	3,570	18.8
B	Soil-cement	1	2 × 2 × 14 ga.	17.7	1,000	0.922	1	16.3	2.9/0.75 = 3.87	526	530	4,430	8.4
C1	Lime	7/8	17 ga. woven wire	17.7	600	0.791	0.729	10.2	2.9/0.75 = 3.87	329	330	3,170	9.6
C2	Lime	7/8	2 × 2 × 14 ga.	17.7	600	0.791	1	14.0	2.9/0.75 = 3.87	452	450	3,940	8.8
D1	Cement-lime	7/8	17 ga. woven wire	17.7	1,000	0.910	0.729	11.7	2.9/0.75 = 3.87	379	380	3,480	9.2
D2	Cement-lime	7/8	2 × 2 × 14 ga.	17.7	1,000	0.910	1	16.1	2.9/0.75 = 3.87	519	520	4,250	8.2
E1	Cement	7/8	2 × 2 × 14 ga.	17.7	1,400	0.946	1	16.7	2.9/0.75 = 3.87	540	540	4,510	8.4
E2	Cement	1.5	2 × 2 × 14 ga.	17.7	1,400	0.989	1	17.5	2.9/0.9 = 3.22	677	680	5,550	8.2

Note: 1 in. = 25.4 mm; 1 kip = 4.448 kN; 1 ksi = 6.895 MPa; 1 lbf/ft = 14.59 N/m.

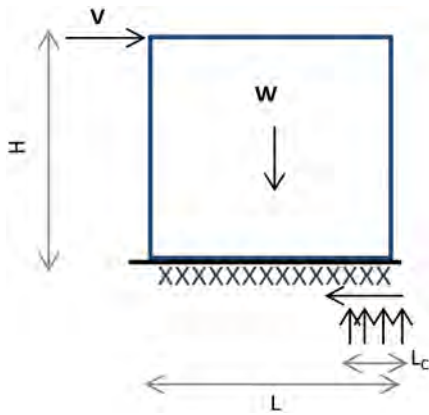


Fig. 8. Rocking model

### Residual Strength Associated with Rocking

Clay plaster designation A1 contains no reinforcing mesh. Its resistance to lateral load is dominated by the resistance to rocking afforded by its self-weight. Self-weight was estimated assuming the average plaster thickness is 1/4 in. (6.4 mm) greater than the specified minimum thickness of 1-1/2 in. (38.1 mm). To be conservative, possible superimposed load was assumed to be zero. Using the model of Fig. 8, a uniform bearing length,  $L_c$ , was determined for plaster cube strengths of 290 and 100 psi (1.99 and 0.69 MPa), to generate a vertical reaction at the base of the wall equal to the self weight of the wall,  $W$ . For this free body diagram, the associated lateral force,  $V$ , required to cause tipping was determined. The change in cube strength from 290 to 100 psi (1.99 to 0.69 MPa) was determined to result in a tipping strength equal to 93.68% of the lateral strength of 1.36 kips (6.05 kN) determined in this analysis.

### Adjustments for Uncertainty

Even though uncertainty related to test data and sample size is addressed in some methodologies [such as the FEMA (2009) methodology for establishing seismic design parameters], allowable shears were further reduced where some uncertainty was present in expected strengths owing to the limited number of full-scale tests. Where full-scale tests reflected the particular plaster types, thicknesses, and reinforcement called for in the model code provisions, a 10% reduction in allowable shear was applied. Where strain-compatibility analyses (e.g., moment curvature analyses using the program *BIAX*) were used to account for changes in plaster strength, thickness, or reinforcement; a 25% reduction in allowable shear was applied. These reductions, included in Column 10 of Table 1, serve to increase the effective factor of safety to the values shown in this column. One exception was made, for the unreinforced clay plaster (plaster designation A1). The lateral strength for this plaster is based on self-weight providing resistance to overturning. Because the overturning capacity is based on weight and geometry, for which relatively little uncertainty exists, the allowable shear was reduced by only 10%. The proposed allowable shears are given to two digits of precision, in tens of pounds per linear foot (Table 1).

### Wall Aspect Ratio

Walls having larger height to length ratio will also fail in flexure. Thus, the allowable shear for such walls should be determined

based on reductions in flexural strength associated with the dimensions of the wall. For walls with reinforced plaster, flexural strength,  $M$ , can be taken as approximately proportional to steel area times plan length,  $L$ . Because steel area is given by a nominal reinforcing ratio,  $\rho$ , times the cross sectional area of the wall, for walls of uniform plaster thickness,  $M \propto \rho L^2$ . By statics,  $V \propto M/h \propto \rho L^2/h$ , where  $h$  is the height of the wall. The corresponding unit shear,  $V/L$ , is proportional to  $\rho L/h$ . That is, the unit shear should be reduced by multiplying by  $L/h$  for walls having  $L/h$  less than 1. That this relationship is conservative is confirmed by the wall tested by Faurot et al. (2004). That 4-ft (1.22-m) long wall had a lateral strength of 7.37 kips (32.8 kN) or 1,840 lbf/ft (26.9 kN/m). This exceeds the expectation of  $2,380(4/8) = 1,190$  lbf/ft ( $34.7(1.22/2.44) = 17.4$  kN/m). The higher lateral strength was attributed by Faurot et al. (2004) to the additional steel reinforcement present where the mesh was overlapped.

A similar analysis applies to the one unreinforced plaster wall. The rocking moment,  $M$ , is proportional to the product of self weight and length. Self weight is also proportional to length. Thus,  $M \propto L^2$ . Then,  $V \propto M/h \propto L^2/h$ . Thus, the corresponding unit shear,  $V/L$ , is proportional to  $L/h$ , just as for the walls with reinforced plasters.

### Shear Strength Estimates

The wall tested by Nichols and Raap (2000) failed in shear at a strength of 36,835 lbf (164 kN). A simple estimate of the strength approached from the perspective of ACI (2011) treatment of reinforced concrete walls considers the nominal shear strength,  $V_n$ , to be composed of concrete,  $V_c$ , and steel,  $V_s$ , components, where, for a squat wall (having aspect ratio of 1:1) in Imperial Units:

$$V_c = 3\sqrt{f'_c} \cdot b_w d = 3\sqrt{0.8 \cdot 1220} \cdot (2.375)(0.8 \cdot 103) = 18,341 \text{ lbf}$$

$$V_s = A_v f_y d/s = (0.9 \cdot 330 \cdot 2)(0.8 \cdot 103)/2 = 24,473 \text{ lbf}$$

$$V_n = V_c + V_s = 18,341 + 24,473 = 42,815 \text{ lbf}$$

where  $b_w$  = the sum of the plaster thicknesses on each side ( $1.125 + 1.25 = 2.375$  in. = 60.3 mm),  $d$  may be taken as 0.8 times the plan length of the wall (8 ft-7 in. = 2.62 m),  $f'_c$  = compressive strength of plaster (taken as 80% of the cube strength of 1,220 psi or 8.41 MPa),  $A_v f_y$  = yield strength of wire reinforcement [taken equal to 90% of the ultimate strength of 330 lbf or 1.47 kN for 16-gauge (1.59-mm) mesh from Parker et al. (2006)] and  $s$  = horizontal distance between vertical wires of mesh (2 in. = 51 mm). This simple calculation estimates a strength of 42,815 lbf (190 kN), equal to 116% of the measured shear strength (36,835 lbf or 164 kN). (In SI units, the preceding equations are

$$V_c = 0.249\sqrt{f'_c} \cdot b_w d = 0.249\sqrt{0.8 \cdot 8.41} \cdot (60.3)(0.8 \cdot 2620) = 81,666 \text{ N} = 81.7 \text{ kN}$$

$$V_s = A_v f_y d/s = (0.9 \cdot 1.47 \cdot 2)(0.8 \cdot 2620)/51 = 108.7 \text{ kN}$$

$$V_n = V_c + V_s = 81.7 + 108.7 = 190.4 \text{ kN}$$

This approach was used to estimate shear strengths of the various plasters, assuming cube strengths equal to the minimum values in the proposed provisions, given in Column 6 of Table 1. 86% (=  $1/1.16$ ) of the values calculated by the above approach are provided in Column 13 of Table 1). In no case was there an indication that the changes in plaster thickness, strength, or mesh would result in shear failures at loads less than those required to develop

**Table 2.** Allowable Shear (Pounds Per Foot) for Plastered Straw-Bale Walls

Wall designation	Plaster (both sides) <sup>a</sup>		Sill plates (nominal size) (in.) <sup>b</sup>	Anchor bolt spacing (on center) <sup>c</sup> (in.)	Mesh <sup>d</sup> (in.)	Staple spacing (on center) <sup>e</sup> (in.)	Allowable shear (lbf/ft) <sup>f,g,h</sup>
	Type	Thickness (minimum, each side) (in.)					
A1	Clay	1.5	2 × 4	32	None	None	60
A2	Clay	1.5	2 × 4	32	2 by 2 high-density polypropylene	2	140
A3	Clay	1.5	2 × 4	32	2 by 2 by 14 ga <sup>i</sup>	4	190
B	Soil-cement	1	4 × 4	24	2 by 2 by 14 ga <sup>i</sup>	2	530
C1	Lime	7/8	2 × 4	32	17 ga woven wire	3	330
C2	Lime	7/8	4 × 4	24	2 by 2 by 14 ga <sup>i</sup>	2	450
D1	Cement-lime	7/8	4 × 4	32	17 ga <sup>i</sup> woven wire	2	380
D2	Cement-lime	7/8	4 × 4	24	2 by 2 by 14 ga <sup>i</sup>	2	520
E1	Cement	7/8	4 × 4	32	2 by 2 by 14 ga <sup>i</sup>	2	540
E2	Cement	1.5	4 × 4	24	2 by 2 by 14 ga <sup>i</sup>	2	680

Note: 1 in. = 25.4 mm; 1 lbf/ft = 14.59 N/m; section numbers refer to provisions of the model code (Hammer et al. 2013).

<sup>a</sup>Plasters shall conform with Sections 104.4.3 through 104.4.8, 106.7, 106.8, and 106.12.

<sup>b</sup>Sill plates shall be Douglas fir-larch or southern pine and shall be *preservative-treated* where required by the *International Building Code*. Multiply allowable shear value by 0.82 for other species with specific gravity of 0.42 or greater, or by 0.65 for all other species.

<sup>c</sup>Anchor bolts shall be in accordance with Section 106.16.3 at the spacing shown in this table.

<sup>d</sup>Installed in accordance with Section 106.10.

<sup>e</sup>Staples shall be in accordance with Section 106.10.2 at the spacing shown in this table.

<sup>f</sup>Values shown are for aspect ratios of 1:1 or less. Reduce values shown to 50% for the limit of a 2:1 aspect ratio. Linear interpolation shall be permitted for aspect ratios between 1:1 and 2:1. The full value shown shall be used for aspect ratios greater than 1:1, where an additional layer of mesh is installed at the base of the wall to a height where the remainder of the wall has an aspect ratio of 1:1 or less, and the second layer of mesh is fastened to the sill plate with the required stapling, and the sill bolt spacing is decreased with linear interpolation between 1:1 and 2:1.

<sup>g</sup>For walls with a plaster Type A on one side and any other plaster type on the other side, a *registered design professional* shall show transfer of the design lateral load into the stiffer Types B, C, D, or E plaster only, and 50% of the allowable shear value shown for that wall designation shall be used.

<sup>h</sup>These values are permitted to be increased 40 percent for wind design.

<sup>i</sup>16 gauge mesh shall be permitted to be used with a reduction to 0.60 of the allowable shear values shown.

flexural failures. Therefore, the assumption of flexural behavior in walls having a 1:1 aspect ratio is supported across all wall designations in Table 1.

If suitable fasteners are provided at the perimeter of the plaster skins, walls that are significantly longer in plan would be expected to fail in shear rather than flexure. However, as indicated in column 14 of Table 1, the shear strengths of the reinforced plasters are estimated to be 8.2 to 18.8 times the allowable shears (which were based on flexural behavior). Thus, stocky walls are likely to have strength and ductility governed by the characteristics of the perimeter fasteners.

## Plaster Reinforcing and Detailing Requirements

Detailing requirements were developed in accordance with the details used in the test specimens. Plaster types, designations, detailing requirements, and allowable shears proposed for use in model code provisions are provided in Table 2. The data provided are at the allowable stress level and are intended for use for resisting wind and seismic loads.

## Conclusions

Allowable shears were developed on the basis of full-scale experimental test data and subsequent analysis for use in the design of straw-bale walls for resisting wind and seismic loads (Table 1). Although flexural failures developed, the allowable shears are put forward in a unit shear format, parallel to that used for light-framed walls with wood shear panels. Factors of safety were amplified relative to those used for light frame shear walls to

account for the limited number of tests and cases where analysis is more heavily relied upon. Design values and detailing requirements are summarized in Table 2.

Model code provisions (Hammer et al. 2013) have been developed that utilize these allowable shears and detailing requirements. These allowable shears supplement information available in existing codes and guidelines, including an appendix on Straw-Bale Construction in the 2015 International Residential Code.

## References

- American Concrete Institute (ACI). (2011). "Building code requirements for structural concrete, committee 318." *ACI 318*, Farmington Hills, MI.
- Ash, C., Aschheim, M., and Mar, D. (2003). "In-plane cyclic tests of plastered straw bale wall assemblies." Ecological Building Network, Sausalito, CA, ([http://www.ecobuildnetwork.org/images/PDFfiles/strawbale\\_code\\_support/inplanecyclicsbwalls\\_illinois2001.pdf](http://www.ecobuildnetwork.org/images/PDFfiles/strawbale_code_support/inplanecyclicsbwalls_illinois2001.pdf)) (May 31, 2014).
- Consortium of Universities for Research in Earthquake Engineering (CUREE). (2004). "Recommendations for earthquake resistance in the design and construction of woodframe buildings." *Publication W-30a*, Richmond, CA.
- Faurot, S., Kelly, K., and Kim, H. (2004). "In-plane cyclic straw bale shear wall testing." *Senior Project Rep.*, California Polytechnic Univ., San Luis Obispo, CA, ([http://www.ecobuildnetwork.org/images/PDFfiles/strawbale\\_code\\_support/inplanecyclicsbwall\\_calpoly2004.pdf](http://www.ecobuildnetwork.org/images/PDFfiles/strawbale_code_support/inplanecyclicsbwall_calpoly2004.pdf)).
- FEMA. (2009). "Quantification of building seismic performance factors." *Rep. No. FEMA-P695*, Washington, DC.
- Hammer, M. (2006). "The status of straw-bale codes and permitting worldwide." *The Last Straw*, Paonia, CO, (<http://thelaststraw.org/>).
- Hammer, M., Aschheim, M., Donahue, K., and Smith, D. (2013). "Recommended building code provisions for engineered strawbale

- construction.” California Straw Building Association, ([http://www.ecobuildnetwork.org/images/PDFfiles/strawbale\\_code\\_support/RecommendedProvisions\\_EngSBCConstruction.pdf](http://www.ecobuildnetwork.org/images/PDFfiles/strawbale_code_support/RecommendedProvisions_EngSBCConstruction.pdf)) (Jun. 4, 2014).
- Jalali, S., Aschheim, M., Hammer, M., and Donahue, K. (2013). “Seismic design factors and allowable shears for strawbale wall assemblies.” Working Draft, ([http://www.ecobuildnetwork.org/images/PDFfiles/strawbale\\_code\\_support/SeismicDesignFactorsAllowShears\\_SBWalls.pdf](http://www.ecobuildnetwork.org/images/PDFfiles/strawbale_code_support/SeismicDesignFactorsAllowShears_SBWalls.pdf)) (Jun. 4, 2013).
- King, B., et al. (2006). *Design of straw bale buildings: The state of the art*, Green Building Press, San Rafael, CA.
- Nichols, J., and Raap, S. (2000). “Straw bale shear wall lateral load test.” *Senior Project Rep.*, Dept. of Architectural Engineering, California Polytechnic Univ., San Luis Obispo, CA, ([http://www.ecobuildnetwork.org/images/PDFfiles/strawbale\\_code\\_support/inplanemonotonicsbwall\\_calypoly2000.pdf](http://www.ecobuildnetwork.org/images/PDFfiles/strawbale_code_support/inplanemonotonicsbwall_calypoly2000.pdf)) (May 31, 2014).
- Parker, A., Aschheim, M., Mar, D., Hammer, M., and King, B. (2006). “Recommended mesh anchorage details for straw bale walls.” *J. Green Build.*, 1(4), 141–151.
- Ramírez, J. C. (1999). “Cyclic in-plane testing of post and beam walls with straw-bale in-fill and stucco/plaster.” M.S. thesis, Univ. of Washington, Seattle, Washington.
- Vardy, S. P. (2009). “Structural behaviour of plastered straw bale assemblies under concentric and eccentric loading.” Doctoral thesis, Queen’s Univ. Kingston, ON, Canada.
- Wallace, J. W. (1992). “BIAX: Revision 1, a computer program for the analysis of reinforced concrete sections.” *Rep. CU/CEE-92/4*, Clarkson Univ., Potsdam, NY.